Galileo Electro-Optics Corporation

Galileo Park

Sturbridge, MA   01518

CURVED CHANNEL MCP IMPROVEMENT PROGRAM

NASA Contract No. NAS5-30047

Final Report

Submitted by: Bruce N. LaPrade

Prepared by: Michael B. Corbett

Date: November 12, 1987

SMALL BUSINESS INNOVATION RESEARCH PROGRAM
PROJECT SUMMARY

Technical Abstract: This is the final report on SBIR Phase I Project. Blowholes and blemishes were determined to originate at two stages of manufacturing. Spherical blowholes resulted from trapped gas between the high melting temperature bond glass and the MCP wafer. During thermal processing, the trapped gas expanded and displaced the softened channel glass to form a spherical inclusion. This defect was eliminated by grinding the prefritted bond wafer and channel plate wafer to a flatness which ensured intimate contact prior to fusion.

Elliptical blowholes or blemishes were introduced during the fiber draw stage. Contaminants trapped between the core bar and clad tubing volatilized providing large quantities of expanding gas. These pockets of gas became elongated to an ellipsoidal shape during fiber draw.

Special cleanliness procedures were developed for the grinding, polishing, and acid-etching of core bars. These provided near contaminant free surfaces which fused into a nearly inclusion free fiber. Wafers manufactured using these fibers have a reduced number of blemishes.

Improvements in channel curvature fabrication were implemented. Incomplete three-ply bonding was identified as a major contributor to channel curvature non-uniformity. Uniform wafer bonds are now produced using the new frit glass approach.

The design of the shearing fixture was evaluated. The original fixture imparted an off-axis moment to the shearing force which contributed to channel curvature non-uniformity. A new design was developed which eliminated the moment.

The shearing furnace design was evaluated. The furnace produced radial thermal gradients within the wafers which caused variations in channel curvature. Steady state thermal conditions instead of thermal transient conditions were determined to reduce curvature non-uniformity.

Anticipated Benefits/Potential Commercial Applications: Significantly improved image uniformity for iamging and pulse counting intensified systems. These image improvements will be realized through the elimination of channel blemishes and improved channel curvature uniformity in curved channel microchannel plates.

Key Words that Describe the Project: Curved channel microchannel plates, MAMA, blemishes, pulse height distribution.

TABLE OF CONTENTS

1.0 INTRODUCTION

1.1 Objective

The chief objective of this SBIR Phase 1 program was to identify the causes of the two major mechanical fabrication defects, channel curvature and blemishes. These defects seriously impair the performance of curved channel (C^2) microchannel plates, and make them unsuitable for high resolution space exploration applications.

Blemishes in the array encompass the first area of investigation. Blemishes are irregular voids in the matrix glass of the MCP. Blemishes or blow holes are believed to be caused by the volatilization of contamination on the core material during the channel bending process when the wafer is subjected to extreme temperatures and pressures. Their elimination would improve performance of curved channel (C^2) detectors by eliminating dead and hot spots from the image area. In addition, potential cost reduction may be achieved through increased yields.

Channel curvature encompassed the second area of investigation. In order to ensure the high performance of "C^2" plates, it is imperative that the channels be curved to a uniform and sufficient radius. Non-uniform channel

curvature can produce gain variations, localized photocathode degradation, ion feedback induced spurious pulses, non-uniform pulse height distributions, and dynamic range limitations. System calibration is currently only a partial solution to non-uniform channel curvature. Perfect curvature would significantly enhance the performance and potentially lower the cost of curved channel MCP's through increased yields.

2.0 PROGRAM STUDIES

2.1 Types of Blemishes

Initially, all blemished samples from various manufacturing stages were characterized. These samples were evaluated by energy dispersive x-ray analysis and scanning electron microscopy. Blow holes or blemishes were found to occur in all three primary areas of the MCP. (Solid glass border, multifiber boundaries, intra multifiber or single fiber boundaries).

An example of the least common type of blow hole is shown in Photograph 1. This blemish occurs on the rim or solid glass border of the MCP. It is of least concern as it does not affect the channel plate's electrical performance.

The second type of blow hole characterized occurs at the multifiber-to-multifiber boundary. These defects were observed more frequently than the rim type. They ranged in size from 1 - 20 channel diameters. These defects were nearly always circular in nature and appeared to displace solid core material. An example of a multifiber boundary blow hole is given in Photograph 2.
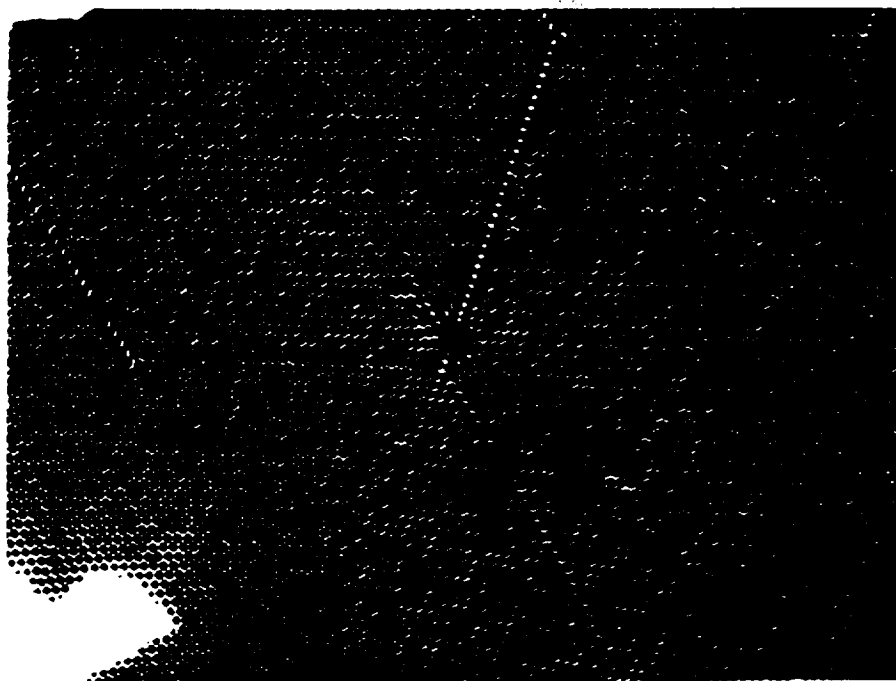
BLOWHOLE IN SOLID GLASS RIM

PHOTOGRAPH 1

BLOWHOLE AT MULTI FIBER BOUNDARY

PHOTOGRAPH 2

The third and most frequently encountered blow hole type was the intra multifiber blow hole illustrated in Photo 3. This type of defect was most easily observed in finished products and almost invariably caused black spots. These defects appeared in the same size ranges as the multifiber boundary blow holes.

2.2 Structure of Blemishes

Examination of blemishes using a high resolution scanning electron microscope revealed that there are two basic shapes, spherical or ellipsoidal. The ellipsoidal blow holes in Photographs 4 and 5 have a large aspect ratio. They are apparently created by the expansion of a gas which forces the rigid core material to be displaced while consolidating the softer cladding. This defect results from voids and inclusions in the drawn single fibers, drawn multi-fibers and fused billets. Airlines or voids can be seen in single fibers, and some bubbles in single fibers were observed to enlarge at temperatures above the sag point. These bubbles can form during any of the forming processes at the glass/glass interface.

Spherical blow holes are found on the surface of curved channel MCPs. Photographs 6 and 7 illustrate this class of blow holes. They are formed when the MCP's are bonded to a

INTRA MULTI BLOWHOLE
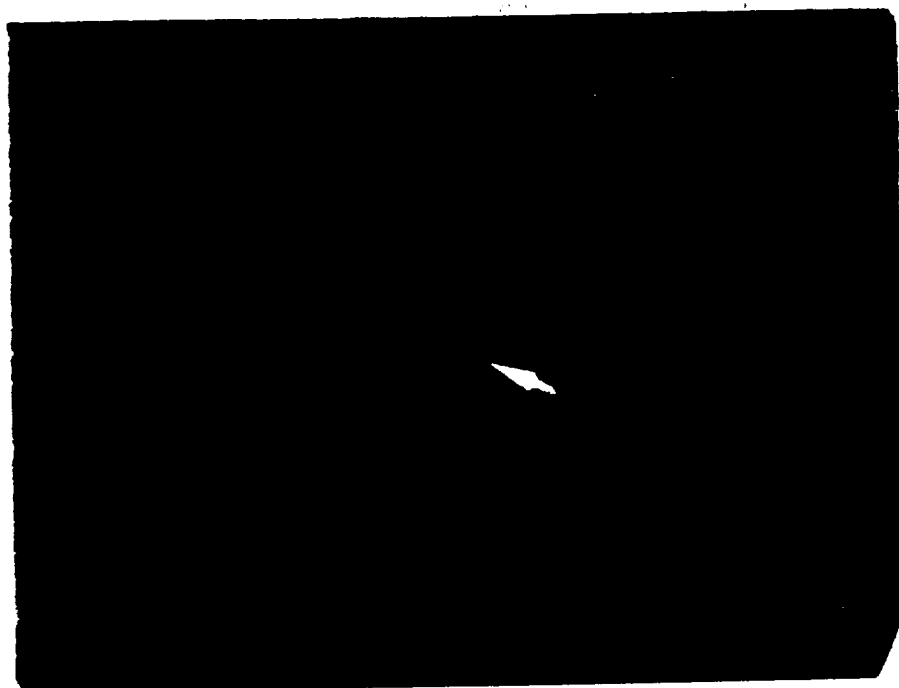
PHOTOGRAPH 3
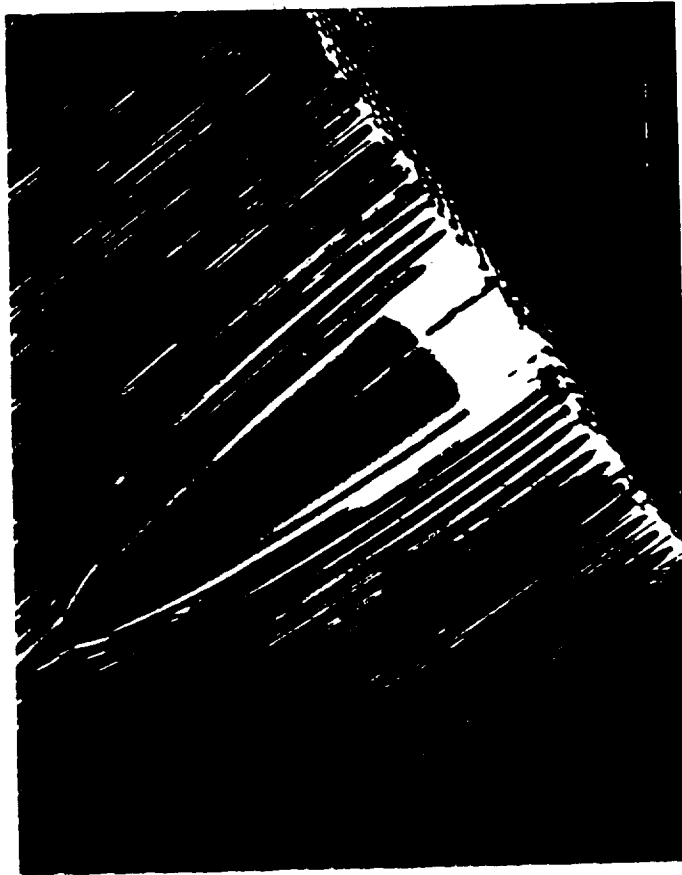
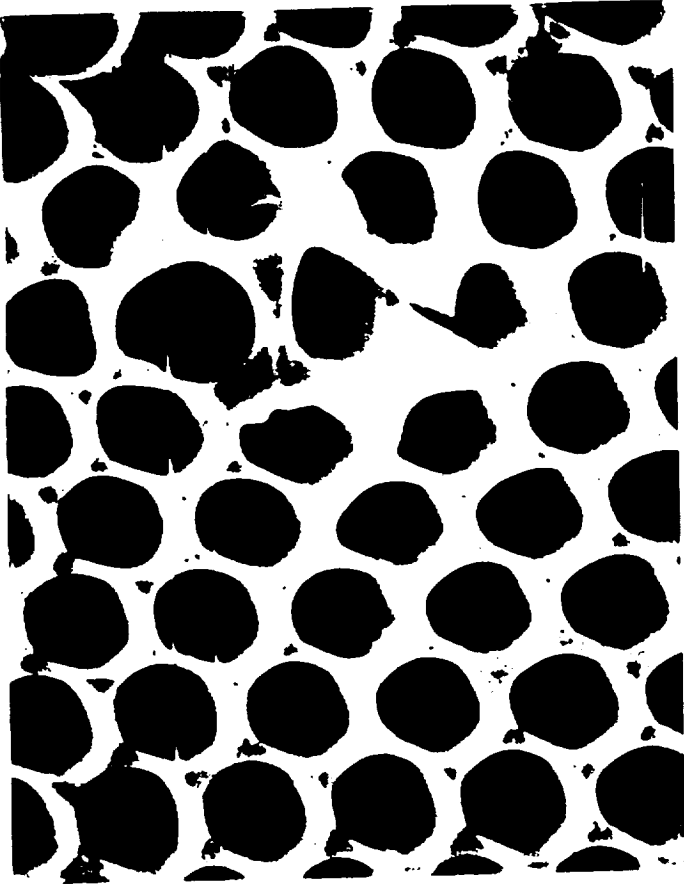CHANNEL WALL DISPLACEMENT BY AN ELLIPSOIDAL BLOWHOLE
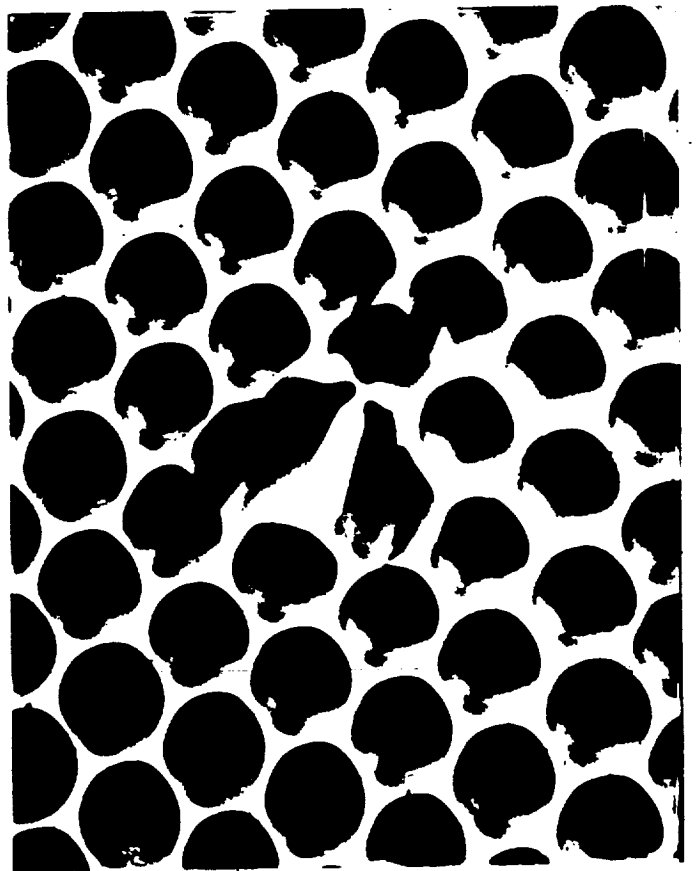
PHOTOGRAPH 4

ELLIPSOIDAL BLOWHOLE

52

SE 250x   10° TiLT   2KU   3/9/87

PHOTOGRAPH 5

PHOTOGRAPHS 6 & 7

SPHERICAL BLOWHOLES

Photograph 6

Photograph 7

harder glass substrate. Any air pockets at the interface form spheres as the MCP part softens. The driving force of this shape change is the reduction in surface energy as the bubble changes from a thin flat shape to a sphere. Spherical blemish formation is now well understood. These blemishes can be eliminated by grinding and polishing the wafers to achieve flatness and void free surfaces.

2.3 Analysis of Blemishes

The study of blowhole morphology identified one source of blemishes. The blowhole surface was studied using energy dispersive x-ray spectroscopy (EDS & EDX). The EDS analysis of the blowhole in photograph 8 revealed a number of contaminants in these blowholes. One EDS spectra was taken in the base glass (Graph 1) and two others were taken in the blow holes (Graphs 2 and 3). The three contaminants found in the blow holes were:

1) Zirconium

2) Iron

3) Carbon

Particulate material was visible in the blow holes having high zirconium and alumina peaks. Zirconia and alumina are used as grinding and polishing compounds. These

11

BLEMISH IN WHICH EDS SPECTRA WAS TAKEN
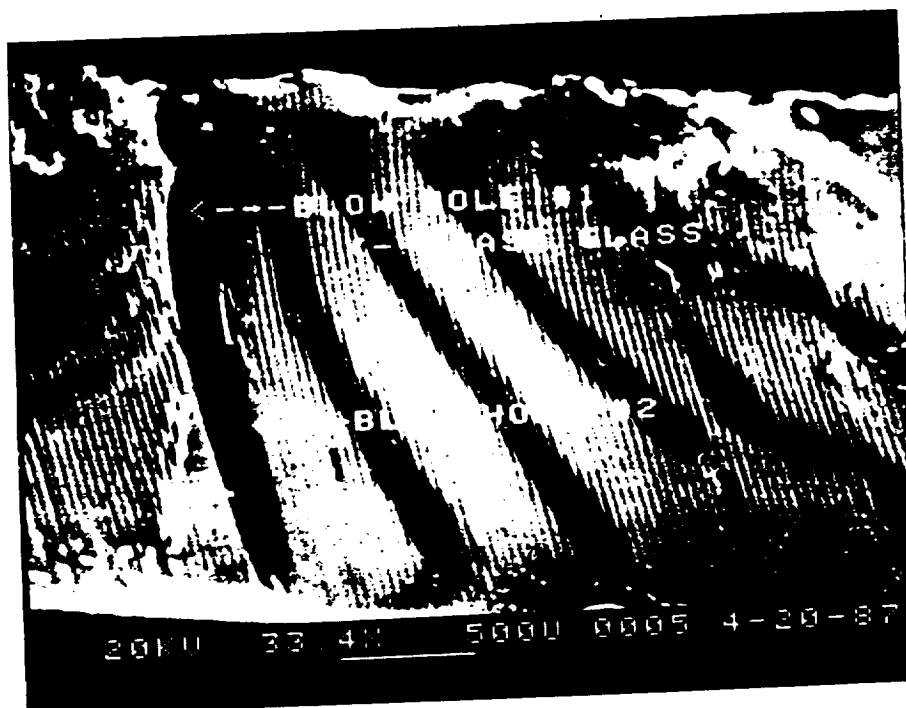
PHOTOGRAPH 8

EDS SPECTRA OF BASE GLASS

30-Apr-1987   : :

BASE GLASS
Vert=   2190 counts Disp= 1

Preset=   50 secs
Elapsed=   50 secs

O

Si

Pb

Al

Ba

Ba

Ba

← 0.000   Range=   10.230 keV

9.950 →
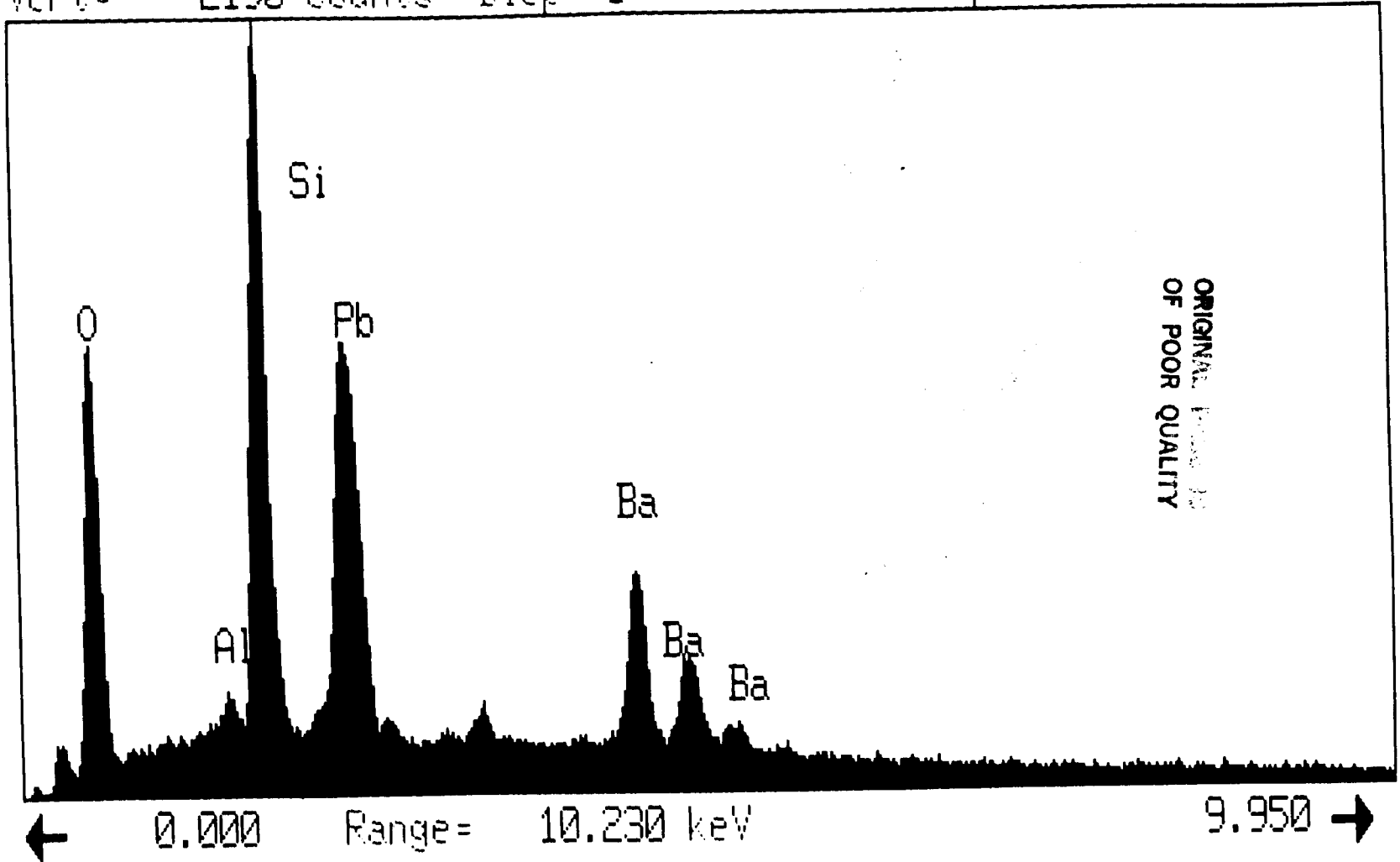
GRAPH 1

EDS SPECTRA TAKEN IN BLOWHOLE

30-Apr-1987   :   :

BLOW HOLE # 1   Preset=   50 secs
Vert=   974 counts   Disp= 1   Elapsed=   50 secs
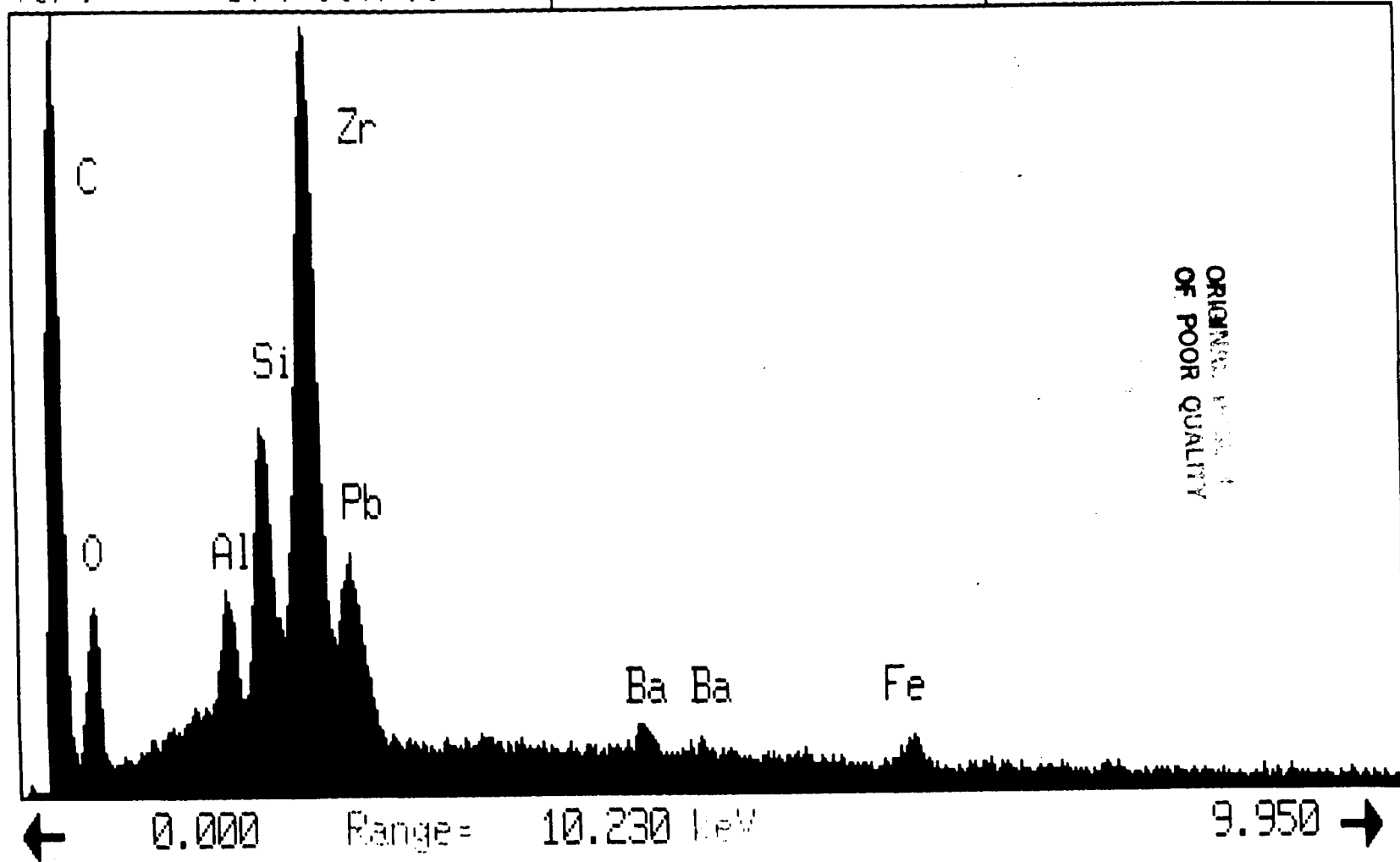
GRAPH 2

EDS SPECTRA TAKEN IN BLOWHOLE

30-Apr-1987   : :

BLOW HOLE #2   Preset=   50 secs
Vert=   2303 counts Disp= 1   Elapsed=   50 secs

Si

Pb

O

Al

Ba Ba

ORIGINAL PAGE IS
OF POOR QUALITY

← 0.000   Range =   10.230 keV   9.950 →
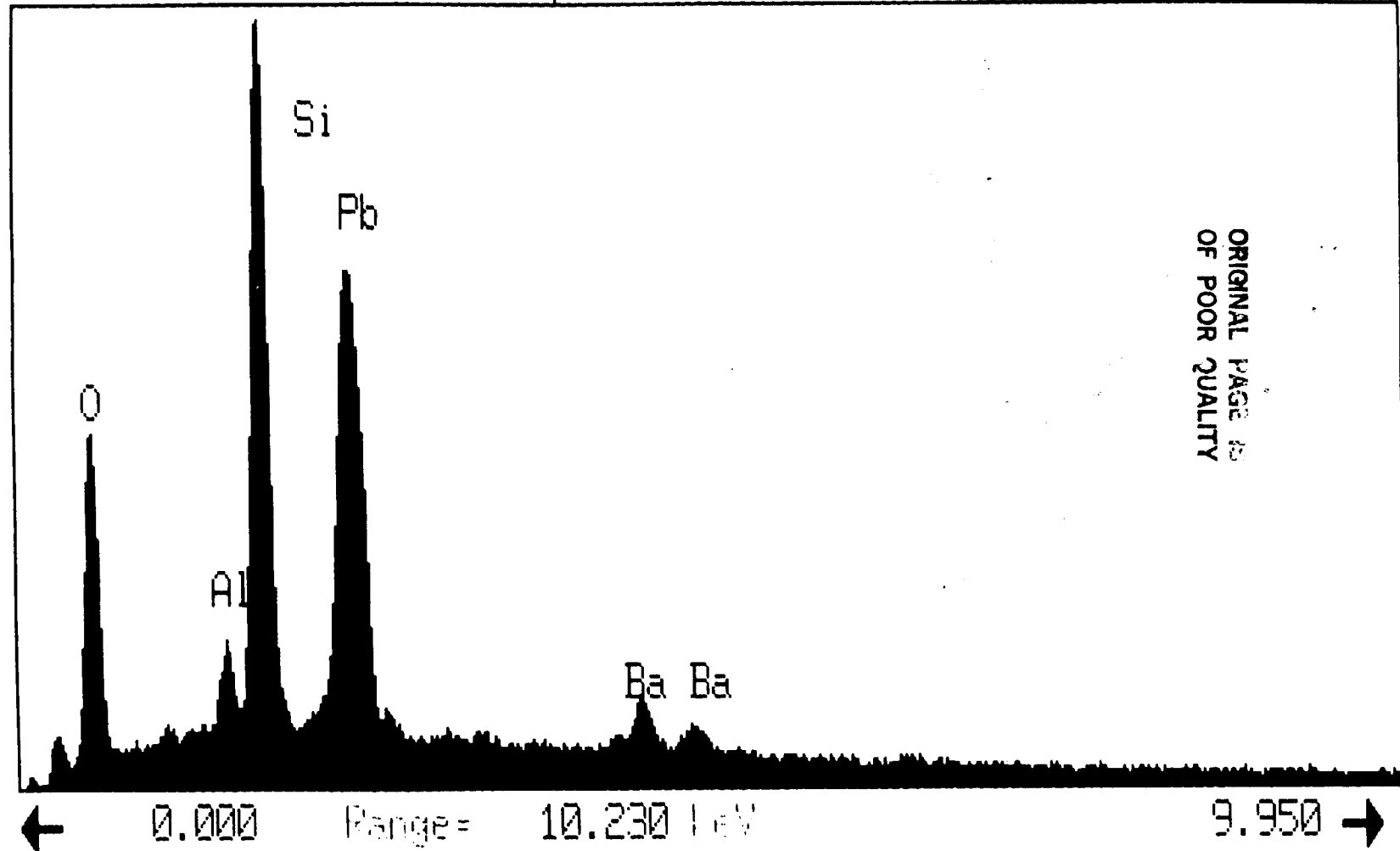
GRAPH 3

contaminants were probably introduced during sample preparation.

The iron peak was found in only one position along the blow hole wall. Iron particles could have been introduced to the MCP during fiber draw, fabrication, finishing, or sample preparation.

The carbon peak was found in a limited area of the blow hole. It occurred only in the area marked "blow hole #1" in Photograph 8. Soft black material has also been found in single fibers. This material appears to be embedded in the glass, Photographs 9 and 10, and most likely was introduced in the high temperature forming operations.

Two other analytical techniques to determine the origin of blemishes were employed. A scanning Auger microprobe was used to analyze the blow hole walls. The non-conductive glass charged during this analysis with no data being obtained. Residual gas analysis was used to identify the gas contained in the blemishes. The volume of gas released from the blemishes was insufficient to analyze.

CARBON INCLUSION STUCK TO GLASS

PHOTOGRAPH 9

CLOSE UP OF CARBON INCLUSION STUCK TO GLASS

PHOTOGRAPH 10

2.4 Channel Curvature

Channel curvature is controlled by the shearing operation. The existing process was studied to identify causes of inadequate curvature. The shearing operation consists of two steps, 3-ply MCP preparation (bonding), and shearing.

The MCP is bonded to a high softening point glass. This glass will not distort at high temperatures. It acts as a rigid support of the MCP, so the MCP will not deform under its own weight at high temperatures.

During the shearing phase forces are applied to a heated 3-ply assembly. The bottom of the 3-ply MCP is held stationary and a shearing force is applied to the face of the MCP (Figure 1). The channels are curved as the top of the channel moves in relation to the bottom of the channel.

2.4.1   Bonding

The first aspect of shearing studied was the bond between the MCP and rigid glass. Examination of sheared plates showed these bonds were not uniform across the MCP face. The rigid glass bonded on the rim, but not on the active area. Photograph 11 shows the separation between the rigid glass

Shearing Schematic

FORCE ➤

V ——▶

Rigid
Glass

◀— MCP

V=0   Q—Heat Flux
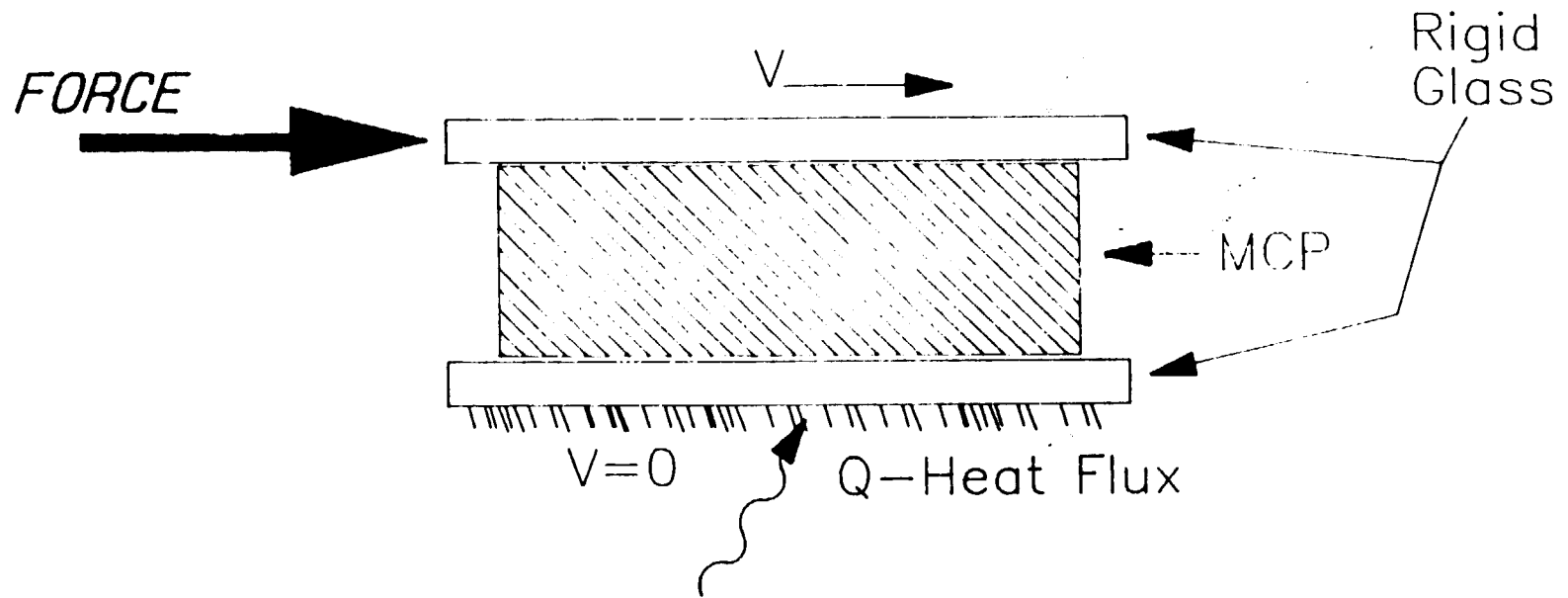
(Fig. 1)

SEPARATION BETWEEN RIGID GLASS AND MCP

PHOTOGRAPH 11

and MCP after shearing. This poor bond results in non-uniform curvature across the MCP face.

The three glasses involved in this bond have different viscosity versus temperature characteristics. Table 1 lists the softening points of the glasses as measured using ASTM C338 54T procedures.

TABLE I

VISCOSITY INFORMATION

Glass	Softening Point ($10^{7.5}$ Poise)
Clad & Rim	642°C
Core	689°C
Rigid	718°C

The softening point of a glass represents the temperature at which that glass will flow under its own weight. A good glass/glass bond requires

some flow of the two glasses involved in the bond. The bonding temperature can be lower than the softening point provided that the glass is under pressure for some period of time.

The three glasses involved in this bond have a wide range of softening point viscosities. The high temperature required to form a good bond between the rigid glass and core glass (660°c) is not practical because of the clad and rim glasses' excessive deformation.

A process was developed to achieve a good bond between the rigid glass and the MCP consisting of the following steps:

1. A low melting (powdered clad/rim glass) layer was bonded to the rigid glass. This bond was made below the sag point of the rigid glass, 660°C, and above the softening point of the frit glass so the frit glass was above its softening point. It flowed and created a very good seal.

2.   The surfaces of the fritted rigid glass and
     the MCP were ground flat to provide intimate
     contact between the two surfaces during
     bonding.

3.   The MCP was partially etched. The etchant
     removed the core glass from the surface of
     the ground surface. Now the MCP had only the
     clad and rim glass for the bonding surface.

4.   A low temperature bond was made between the
     frit glass and the MCP. Only the rim and
     clad glass were involved in this bond.

An example of this bond is shown in Photograph 12.
This photograph illustrates the deformation of the
glass at the interface between the two glasses.

A high quality bond between the rigid glass and
the MCP allows control of the movement of the MCP.
If the bond between the rigid glass and the MCP is
good and the rigid glass is indeed rigid at the
shearing temperatures, the shearing forces will be
constant across the active area of the MCP.

BOND BETWEEN RIGID GLASS AND A MCP USING NEW BONDING PROCEDURE
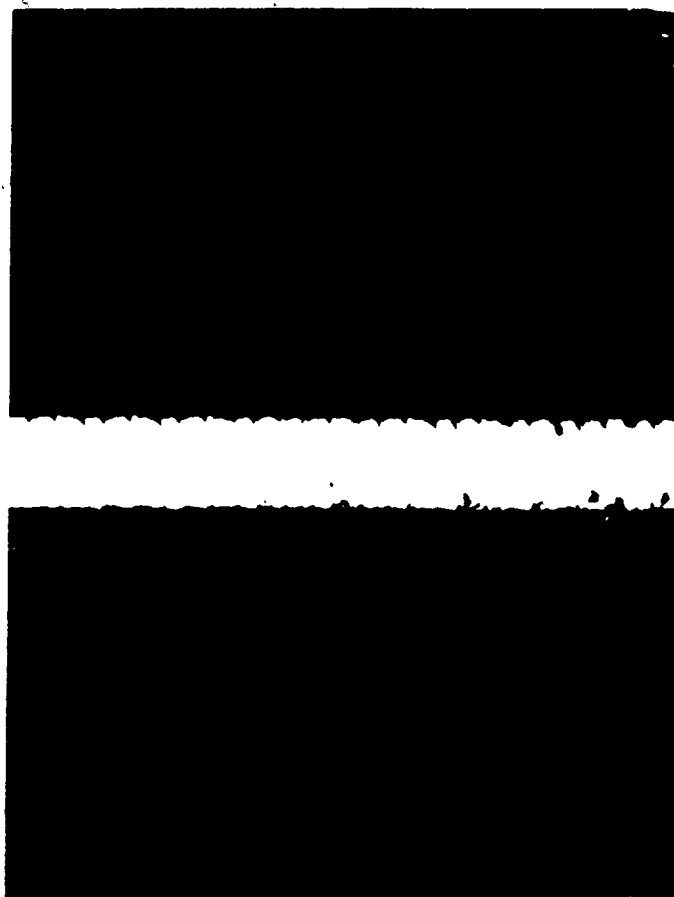
PHOTOGRAPH 12

2.4.2   Shearing

The forces applied to the heating of the 3-ply were investigated. Modifications to the shearing process were evaluated.

2.4.2.1   Shearing Fixtures

The sole purpose of the shearing fixtures is to apply only a shearing force to the MCP. The shearing fixtures did not perform this task. In addition to the shearing force the fixture applied a moment to the MCP. The applied shearing forces in Figure 2 represent what was actually occurring rather than Figure 1.

Figure 3 is a sketch of the old fixture design. Ideally this fixture transfers a vertical force (P) into a horizontal force (S) with a wedge pin and sliding plate. There is some clearance between the machined surfaces, allowing the sliding plate to rotate, and the sliding plate will impart a moment to the 3-ply.

Actual Shearing Forces
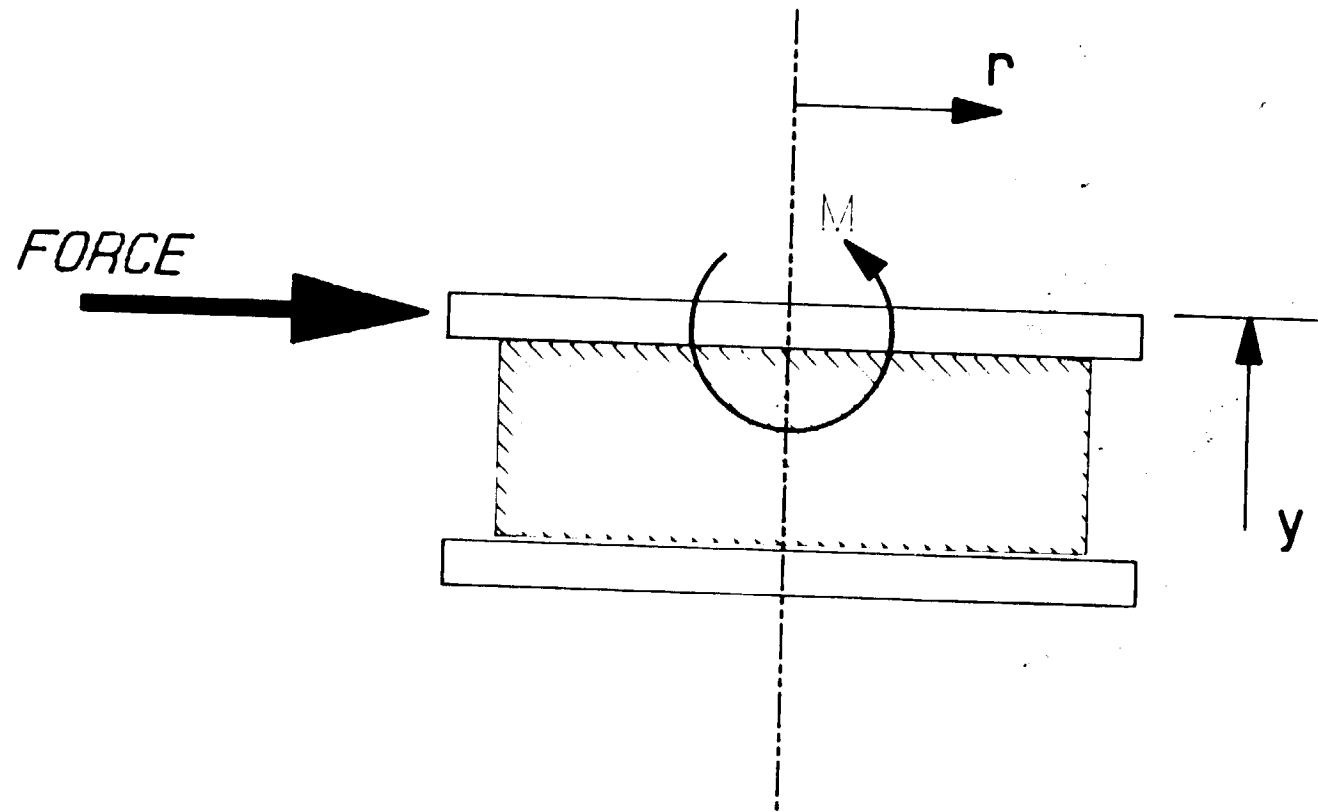
(Fig. 2)

Old Shearing Fixture

P

Wedge

F

S

3-ply

Sliding Plate

Stationary Base
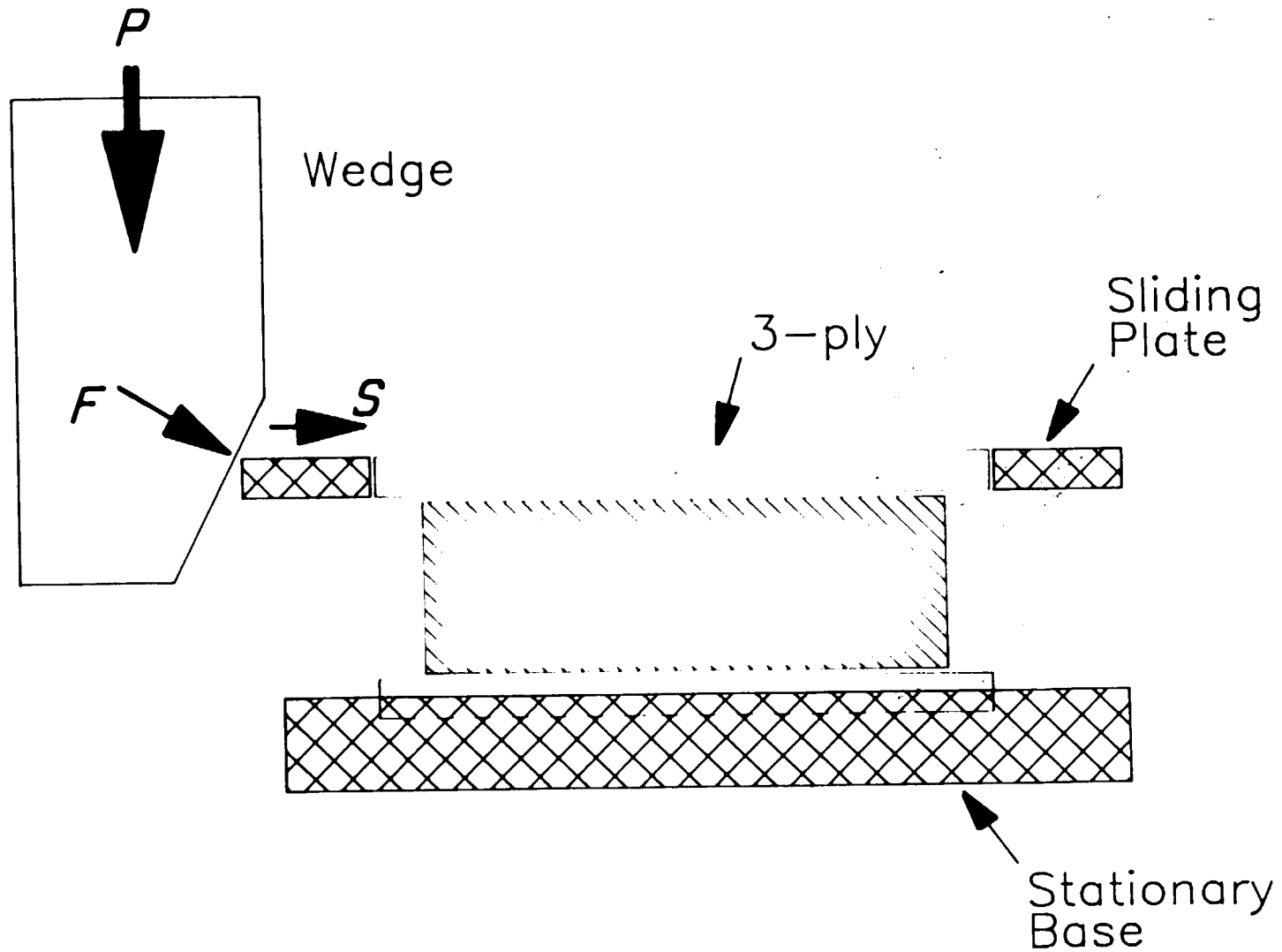
(Figure 3)

Figure 4 shows the modified shearing fixture. In this design the force applied to the fixture is transferred to the 3-ply via the sliding plate. No wedge is necessary to change the direction of the applied force.

2.4.2.2   Thermal Profile

The thermal profile of the MCP during shearing is an extremely important factor. Glass viscosity is a function of temperature, and any changes in viscosity affect the velocity of the glass during shearing. If there is a thermal gradient in the MCP, the glass will not deform at the same rate. This results in uneven curvature if the gradient is in the radial direction (Figure 2 notation).

The thermal profile of an MCP was taken by bonding low mass thermocouples to the MCP. The thermocouples were placed as shown in Figure 5. The resulting temperature profiles are shown in Graphs 4 and 5. These graphs indicate a temperature gradient of 80°C axially, 10°C radially on the bottom and 20°C radially on the top.

New Shearing Fixture

3-ply

Sliding Plate

P
S

Stationary Base

(Figure 4)

Rigid Glass

MCP

Rigid Glass

MCP
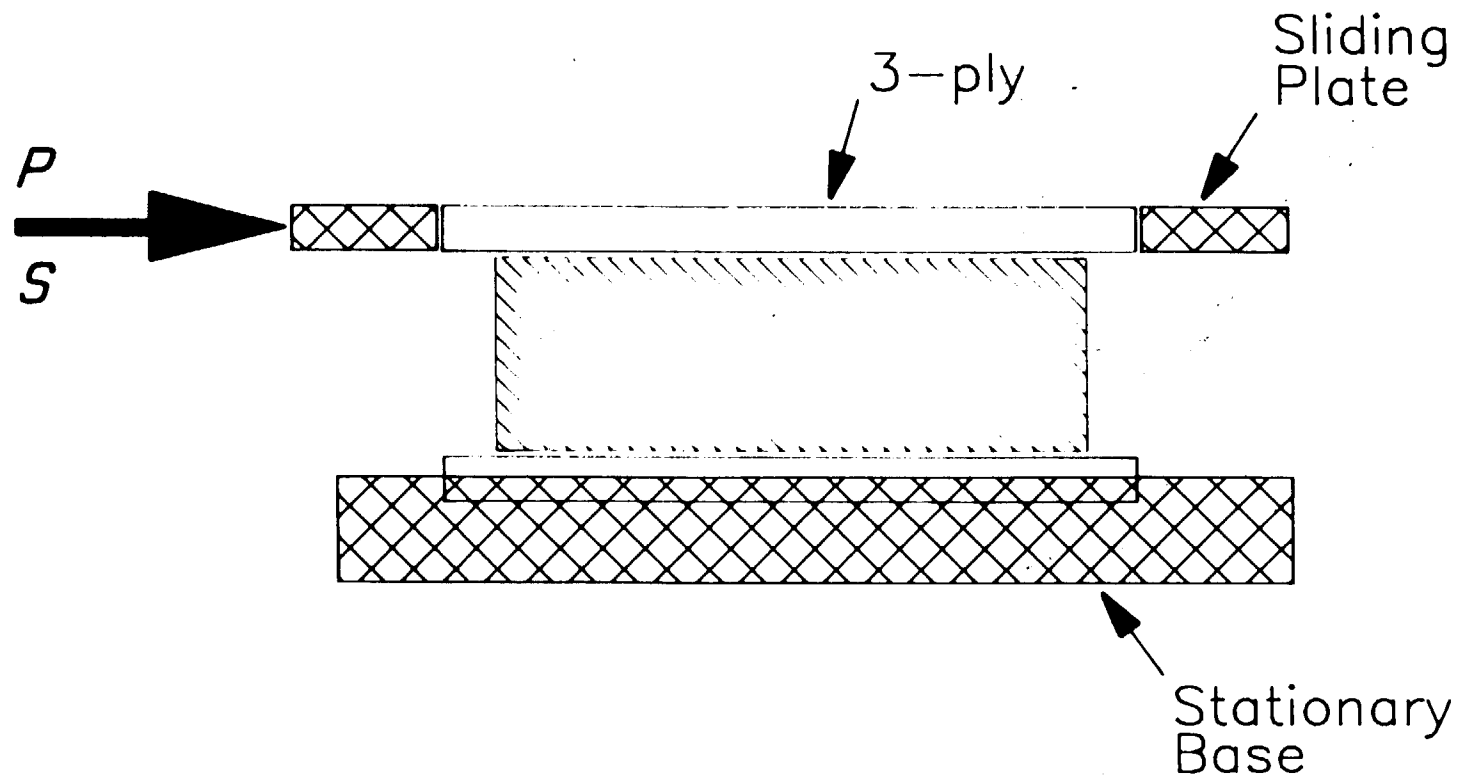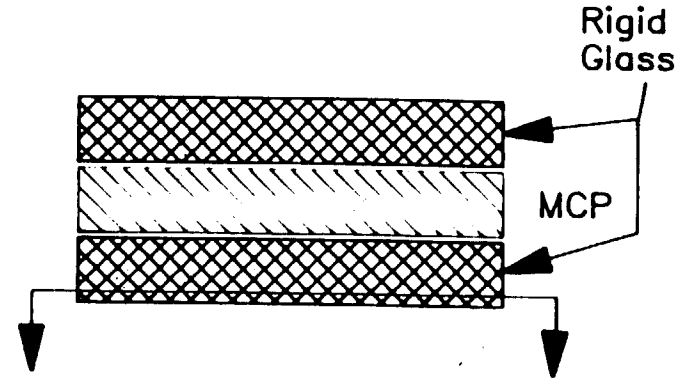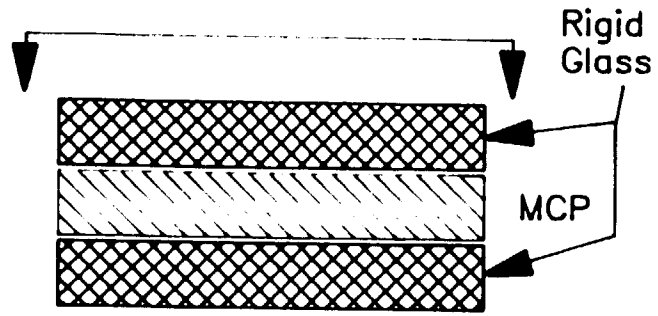
Approximate positions of Thermocouples:

Top:

.38"

.62"

1 ●   ● 3

2 ●

.15"
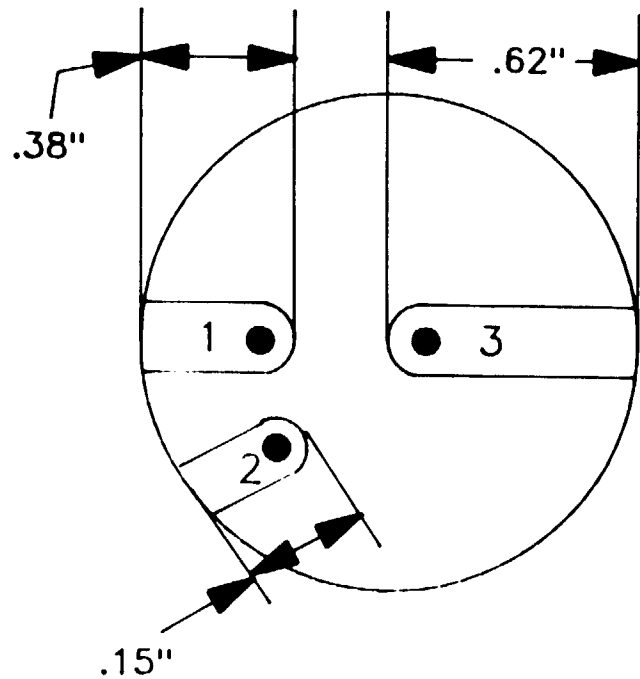
Section of Bottom
(viewed from top):

.33"

.60"

5 ●

6 ●

4 ●

.20"
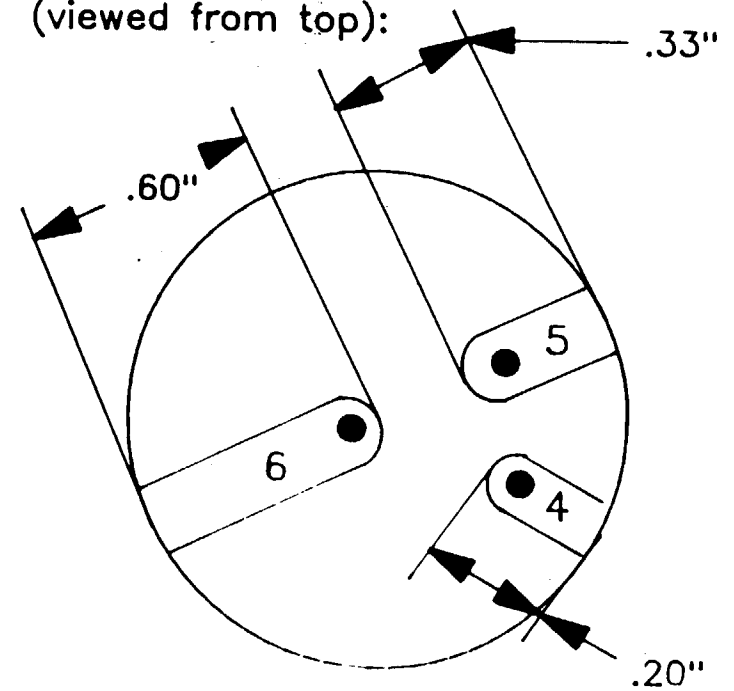
● = Thermocouple

THERMAL MAPPING

25mm MCP 10:05AM 5/28/87

TIME (Minutes)

TEMPERATURE (C)

—— 1   —— 2   — · 3   —— 4   —— 5   —— 6

MCP 11/9/87

THERMAL MAPPING

25mm MCP 10:05AM 5/28/87

TIME (Minutes)

TEMPERATURE (C)

——— 1   ——— 2   — · 3   ——— 4   —·····— 5   ——— 6
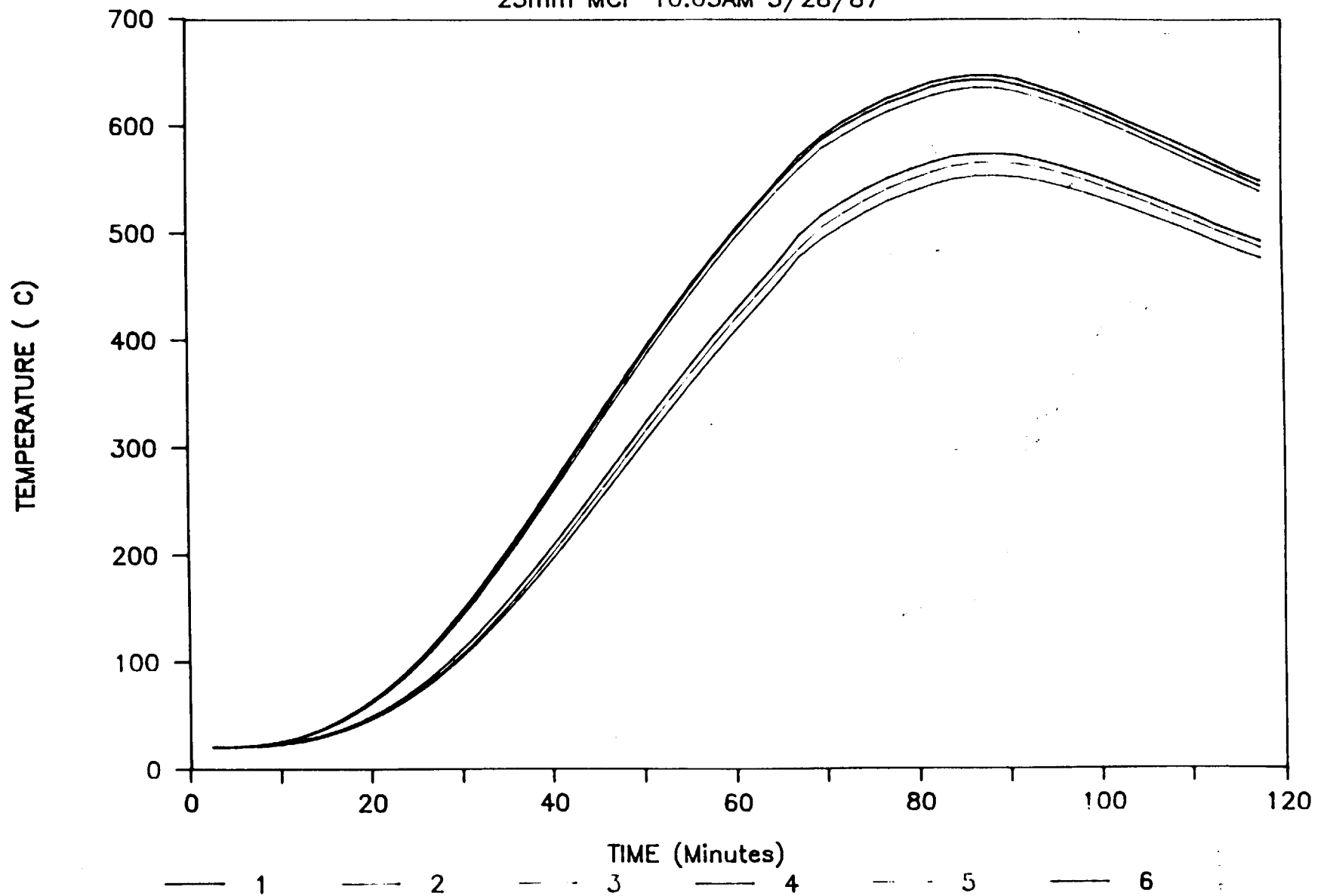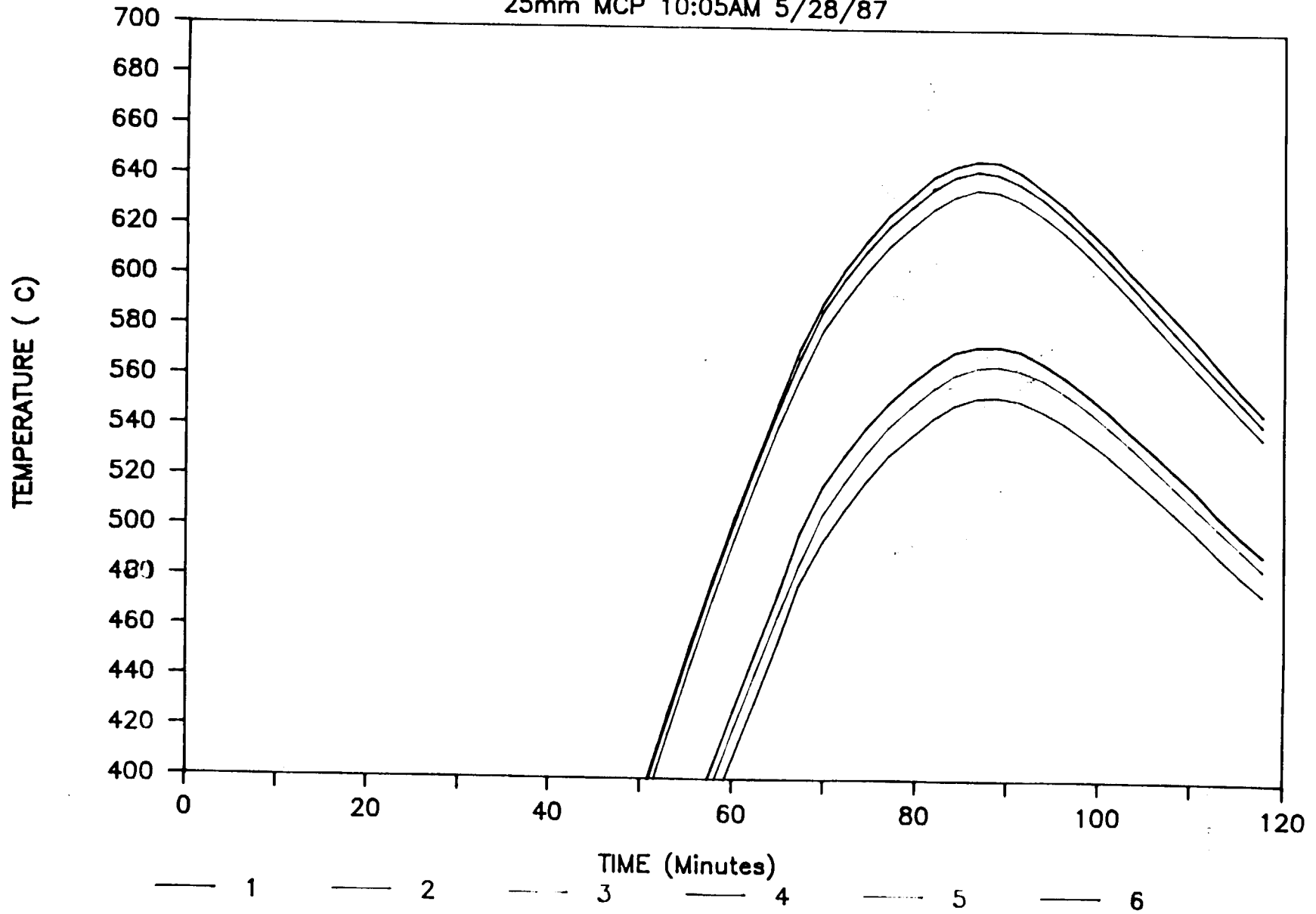
The MCP's are heated by a resistance furnace located below the fixture. The top of the fixture is exposed to air at ambient conditions. The temperature profiles can be attributed to the boundary conditions on the shearing fixture. The radial temperature gradients are less dramatic when thermocouple error is considered, $\pm2.9°C$. It should also be noted that the MCP's are sheared on a thermal transient. Any changes in the initial conditions or the boundary conditions of the shearing fixture and furnace will affect the thermal profile of the MCP. These difficulties could be avoided if the MCP's were sheared under steady state thermal conditions.

2.4.2.3   Shearing Model

Before a new heating scheme can be designed, the optimum temperature profile must be identified. A model which solves the momentum equation for fluid flow was developed. The assumptions made in developing this model are:

1)   There is only a velocity gradient in the y direction. Any velocity gradient due to

boundary effects and radial temperature
gradients were ignored.

2)   The glass is a continuum. This
assumption neglects the fact that the MCP is
a composite material.

3)   The glass behaves like a Newtonian fluid.
Kingery[1] reports that glass behaves like a
Newtonian fluid at viscosities less than
$10^{9.1}$ Poise. Therefore, this shear equation
is applicable:

$$\tau = \eta \frac{du}{dy}$$

4)   The viscosity can be represented by an
exponential function:

$$\eta = A_1 \bullet e^{A_2/T}$$

   where A_2 is the temperature constant.
   (Kingery[1] p758)

This equation was solved for an isothermally
sheared plate, as well as a plate with a
linear temperature gradient through it. The
details of the solution can be found in
Appendix A. This model will predict the
curvature of the channels under various
shearing conditions.

The solution of the momentum equation for an isothermally sheared plate is:

$$u = u_o \frac{y}{l} + 2 u_o \sum_{n=1}^{\infty} \left[\frac{1}{n\pi} \cos n\pi - \frac{1}{l^2} \sin n\pi \right] \sin \frac{n\pi y}{l} \exp \left(- \frac{n^2 \pi^2 \eta}{l^2} t \right)$$

This solution consists of a steady-state portion and a transient portion. The first term is the steady-state solution and the summation is the transient portion of the solution. The transient portion of the solution decays rapidly for this very viscous glass. The half life of the transient is:

$$t_{1/2} = \frac{l^2}{n^2 \pi^2 \eta} \ln .5$$

so the solution is approximately equal to the steady-state solution:

$$U_\infty = u_o \frac{y}{l}$$

The transient has even less effect on the solution for displacement which is the integral of the velocity expression.

The graph of the displacement, Graph 6, predicts that the channels will have no bend in them at all. Photograph 13 shows a MCP which was sheared under isothermal conditions. The channels do show some curvature, however. The discrepancy between the curvature model and the actual channel curvature may be caused by minor temperature gradients in the shearing apparatus or errors due to the assumptions made about the glass.

MCPs are normally sheared with a temperature gradient through them. The temperature gradient for this model was not actually measured. The temperatures of the top and bottom faces were measured. The MCP was assumed to be at thermal equilibrium with a linear temperature gradient like this:
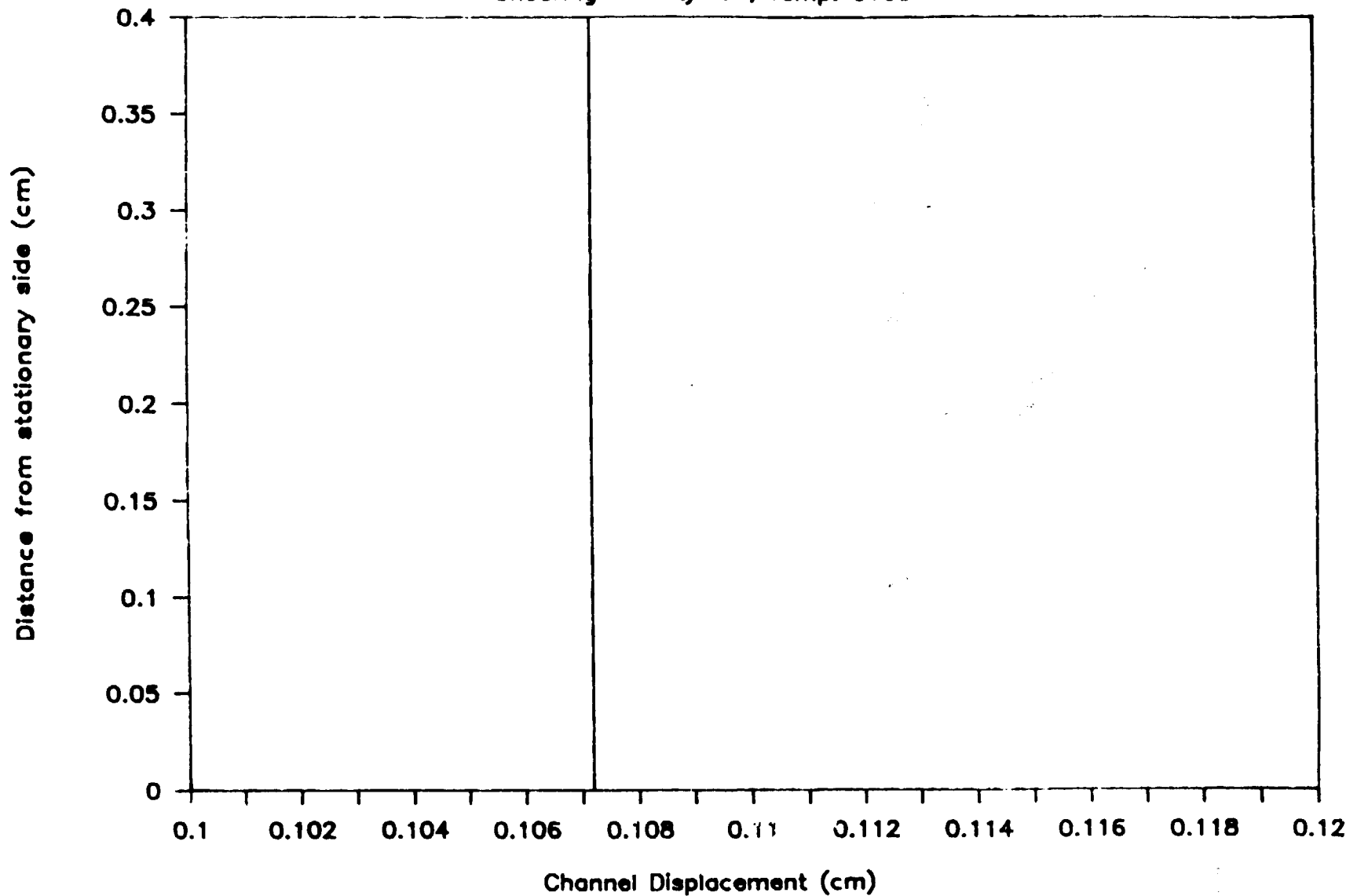
$$T = C_1 y + C_2$$

The steady state solution of the momentum equation for this linear temperature gradient is:

$$u = \frac{A_2}{C_1} \ln |(C_1 y + C_2)| + C_3 y + C_4$$

Channel Curvature @ Constant Viscosity

Shearing Velocity .01; Temp. 610C

Channel Displacement (cm)

GRAPH 6

CHANNEL CURVATURE OF ISOTHERMALLY SHEARED MCP

PHOTOGRAPH 13

The maximum curvature for a given glass and bias angle can be attained by shearing the plates a distance equal to:

shear distance = l·tan (bias angle)

This distance is equal to the projection of a single channel on the flat surface of the MCP. The resulting shape of curvature is a parabolic as seen in Graph 7. Photograph 14 illustrates the near parabolic channel curvature that occurs in a MCP sheared with a 100° thermal gradient across it.

The curvature can be further maximized by increasing the temperature gradient across the MCP. Graph 8 illustrates the effect of an increase in the temperature gradient from 100°C to 200°C.

Increasing the glass's viscosity "temperature constant" (see appendix A for details) will also increase the channel curvature for a given temperature gradient. The curvature increases as the "temperature constant" is doubled for a 100°C temperature gradient (see Graph 9).

Channel Curvature; Linear Temp. Profile

Shear velocity .01 cm/s, TO 520 T4 620C

Shear Velocity .01^{cm}/s

Top Temperature 520°C

Bottom Temperature 620°C

"Temperature Constant" (A$_2$) 38.22

Distance from Stationary side (cm) (y-axis: 0, 0.05, 0.1, 0.15, 0.2, 0.25, 0.3, 0.35, 0.4)

Displacement (cm) (x-axis: 0.1, 0.102, 0.104, 0.106, 0.108, 0.11, 0.112, 0.114, 0.116, 0.118, 0.12)
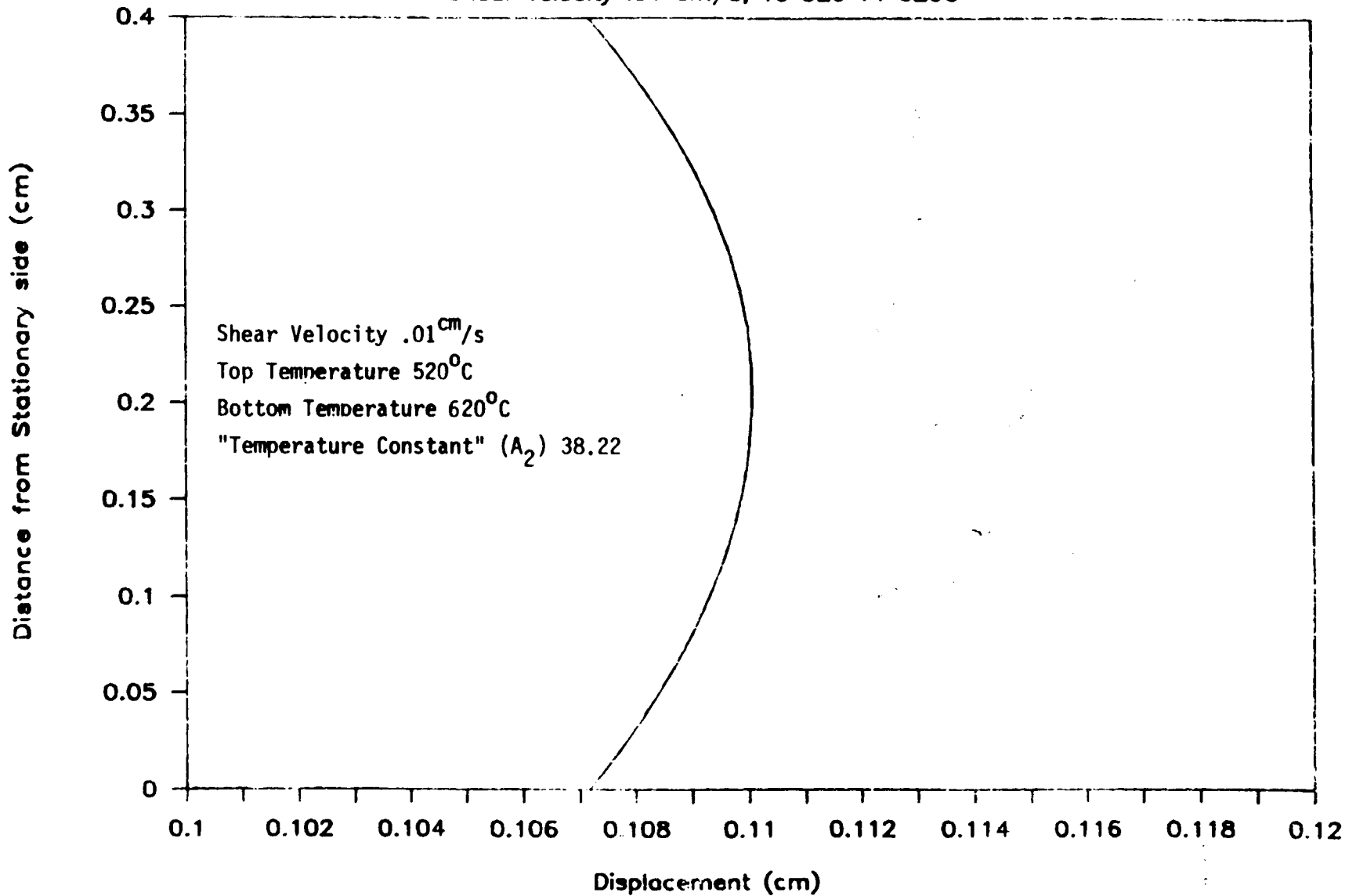
GRAPH 7

ACTUAL CHANNEL CURVATURE OF A MCP SHEARED WITH A 100° TEMPERATURE GRADIENT
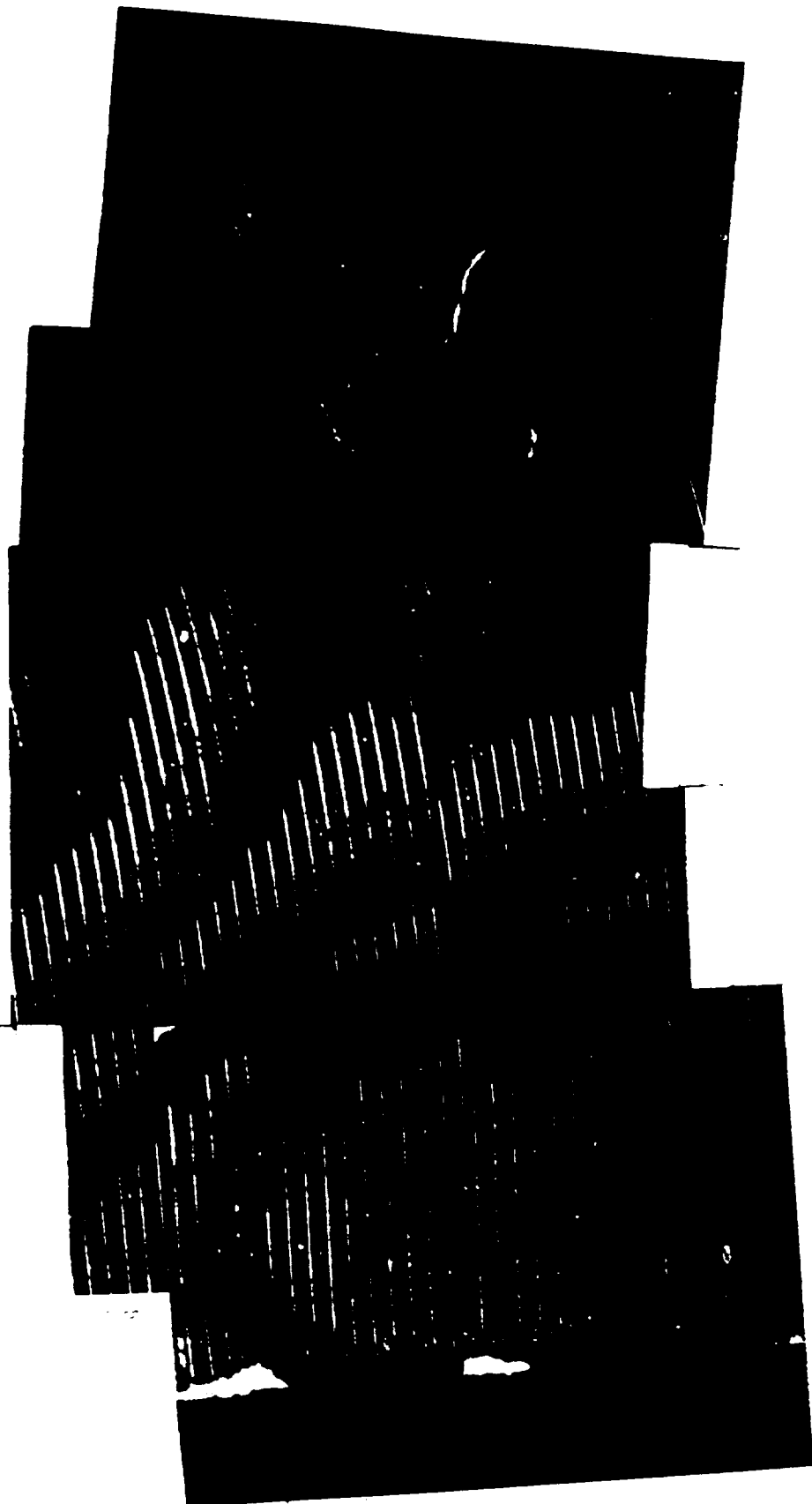
PHOTOGRAPH 14

Channel Curvature; Linear Temp. Profile

Shear Velocity .01^{cm}/s

Top Temperature 520°C

Bottom Temperature 720°C

"Temperature Constant" (A$_2$) 38.22

Distance from Stationary side (cm)

Displacement (cm)
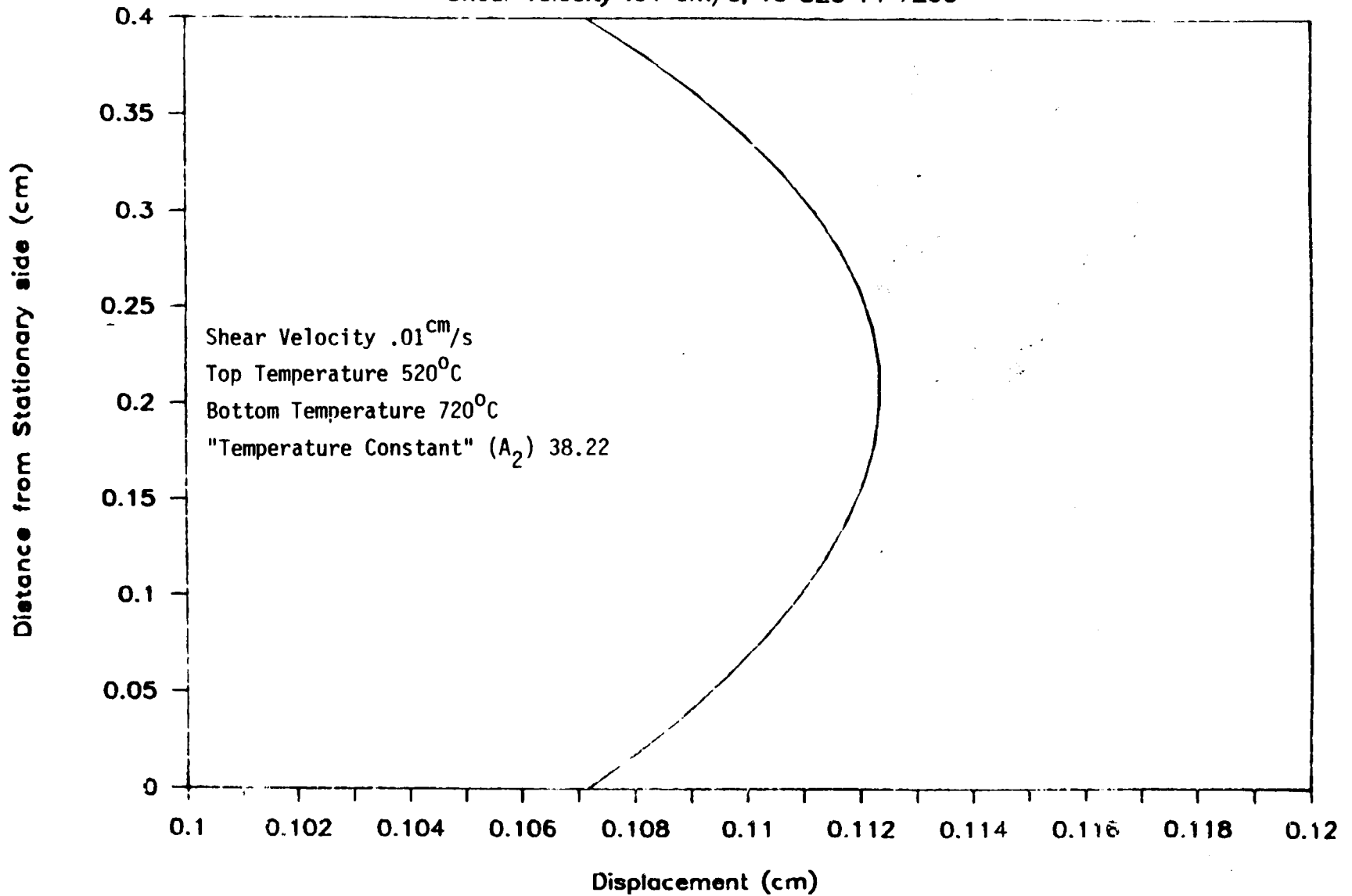
GRAPH 8

Channel Curvature; Linear Temp. Profile

Shear velocity .01 cm/s, TO 520 T4 620C

Shear Velocity .01^{cm}/s
Top Temperature 520°C
Bottom Temperature 620°C
"Temperature Constant" (A$_2$) 85.66

Distance from Stationary side (cm)

Displacement (cm)
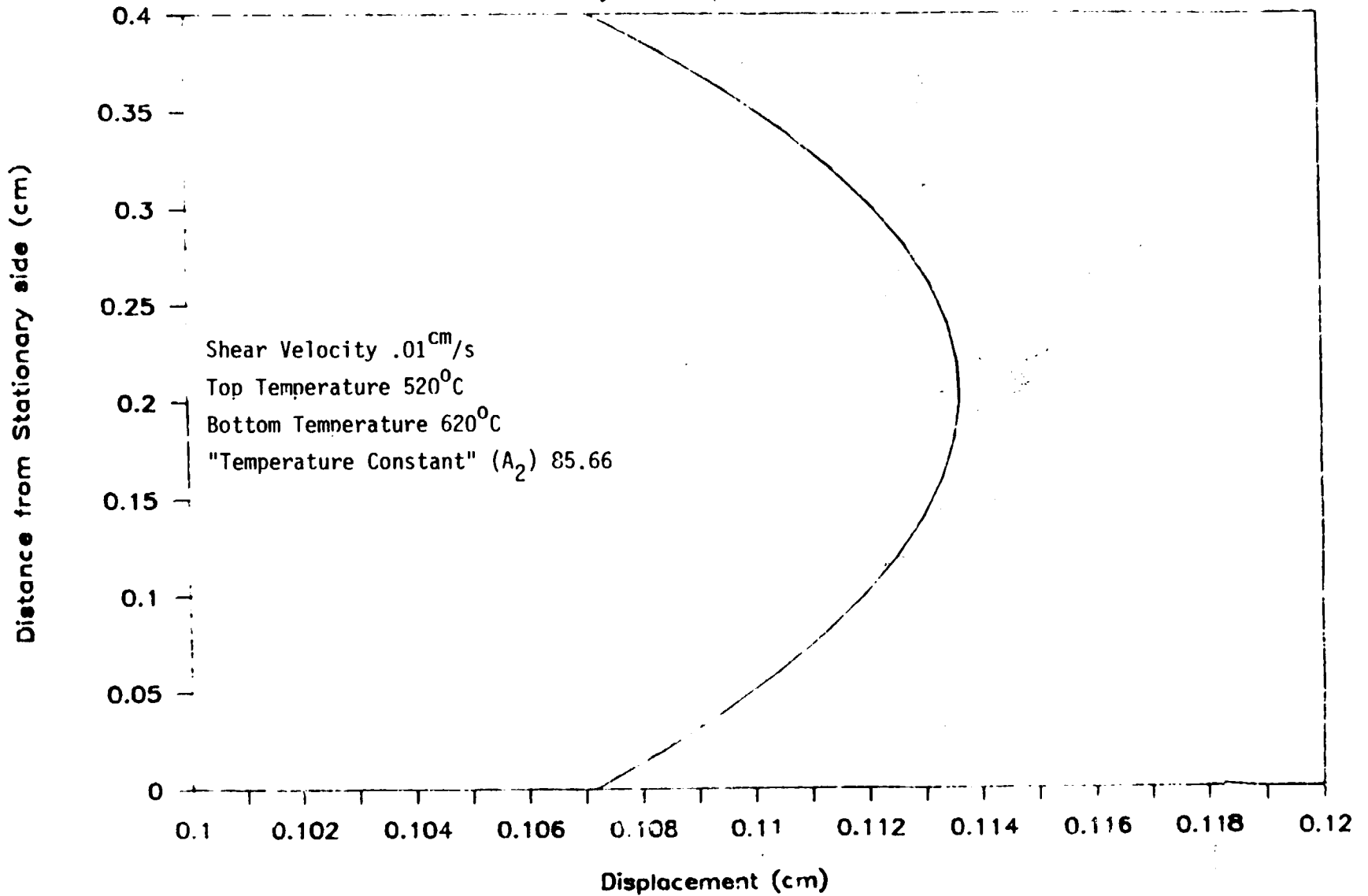
GRAPH 9

## 2.4.3 Comparison of Old and New Shearing Methods

In order to evaluate the modifications to the shearing process, curved channel MCP's that were sheared using both old and new methods were compared by optical scanning. MCP's were selected as representative of the two groups.

Photograph 15 is representative of the plates sheared using the old method. It consists of a series of photographs of a c^2 MCP cross section. This photograph illustrates the channel curvature non-uniformity from one end of the active area to the other. There is no pattern to these curvature variations. Each MCP sheared using the old method has a unique channel curvature pattern.

Photograph 16 represents the MCP's sheared using the modified bonding process and the altered shearing fixture. These MCP's also have non-uniform channel curvature, but this non-uniformity follows the same pattern from plate to plate. The amount of channel curvature decreases from the load point where the shearing force is applied to the unloaded side. The curvature approaches constant radius in the areas furthest from the shearing load. Nearest the shearing load point the curvature resembles a "J" shape or non-constant radius. This change in the channel curvature is most likely caused by the deformation of the rigid glass

45

CROSS SECTION OF A MCP SHEARED USING OLD PROCEDURE
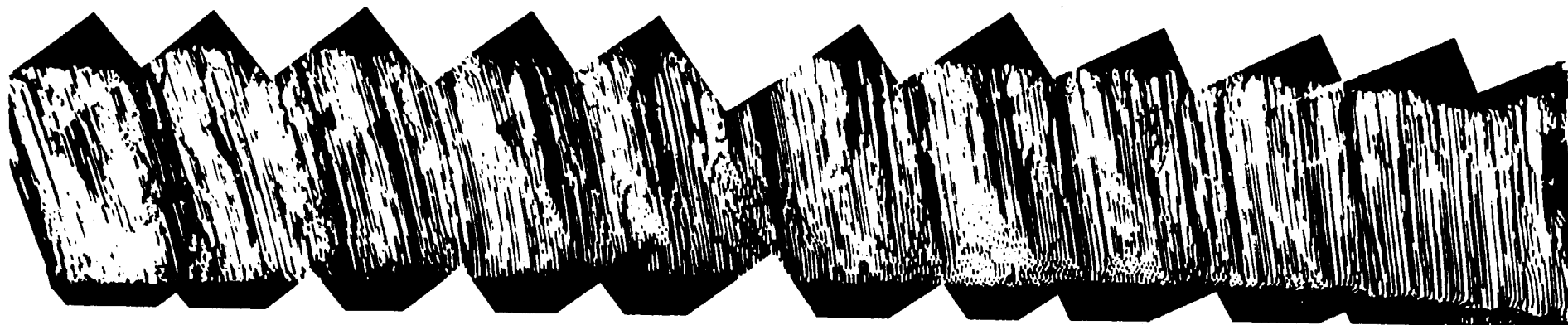
PHOTOGRAPH 15

CROSS SECTION OF A HEP SHEARED USING NEW PROCEDURE

PHOTOGRAPH 16

during the shearing process. Measurements of the 3-ply after shearing indicate that the 3-ply does deform into an elliptical shape during the shearing process. The difference between the major and minor elliptical axes is between .050" and .075".

The new shearing methods significantly improve the channel curvature across the active area. Any residual non-uniformity is apparently caused by the deformation of the rigid glass.

3.0 CONCLUSIONS

3.1 Blemishes

Blemishes occuring during the bonding process can be eliminated by improved surface preparation. Removal of the surface stock by grinding of the MCP and rigid glass eliminates any large blemishes.

The ellipsoidal blemishes are caused by defects in the drawn fiber. The structural data indicates that the defect was elongated during the draw process. EDS analysis indicates that these defects are caused by organic contaminants.

3.2 Channel Curvature

Non-uniform channel curvature can be attributed to deformation of the rigid 3-ply glass, poor bonding of the 3-ply, temperature gradients in the 3-ply and inadequate tooling.

Alternative materials with higher melting points and with coefficients of thermal expansion that match the expansion

of the MCP should be identified as replacements for the rigid glass used in the present shearing process. The ideal rigid material would not deform at high temperatures and would have a high modulus of elasticity at 620°C.

Good bonding was obtained by optimizing the bonding process parameters. The critical parameters of the bonding process are the glass viscosities at the bonding temperature and the surface cleanliness and finish at the bond interface.

Temperature gradients in the 3-ply can be decreased by improving the design of the shearing furnace. Controlling the temperature at the top of the shearing fixture improved channel uniformity.

The shearing fixturing was redesigned so that only a shearing force is applied to the 3-ply. Other fixture parameters identified by the shearing model were incorporated to maximize channel curvature. Channel curvature can further be optimized for a given glass by maximizing the temperature gradient across the MCP, controlling the distance the shearing plate moves and increasing the bias angle.

50

The shearing model indicates that maximizing the viscosity differential across the plate during shearing will increase the channel curvature. This can be effected through increased temperature differential for a given glass or changing to a glass with a steeper viscosity curve.

4.0 RECOMMENDATIONS

Blowholes and blemishes are believed to originate in the fiber draw and redraw operations. Process improvements should be made to eliminate contaminants and defects in the drawn fiber. Specific areas to be improved are cleanliness of draw area, fiber and glass handling and glass preparation.

In the area of channel curvature a number of improvements must be effected. Two of the process steps were addressed under this contract; 3-ply fabrication bonding and fixture design. The temperature gradients during shearing were identified as a critical control parameter. Significant improvement could be achieved with an improved furnace design that would minimize the radial temperature gradients.

APPENDIX A

Shearing Model Derivation

Shearing Model Derivations

The basic equations used for these derivations are written below. They represent the assumptions which are stated in the text:

1) The glass moves in only one direction.

2) The glass is an isotropic continuum.

3) The glass behaves like a Newtonian fluid.

4) The viscosity can be represented by an exponential function.

5) The glass is stationary prior to shearing.

The momentum equation[4]

$$\frac{\partial \rho}{\partial \rho} = (1)\frac{\Delta \rho}{\rho}$$

Newtonian shear equation[3]

$$\tau = \eta \frac{du}{dy}$$

Absolute-Rate viscosity equation[3]

$$\eta = A_1 e^{A_2/T}$$

The momentum equation is solved for two cases constant viscosity and variable viscosity. An additional assumption was made for the variable viscosity case:

6) The temperature gradient is linear across the MCP.

Temperature equation

$$T = C_1 y + C_2$$

Both cases have the same boundary conditions:

$$u(0) = 0$$

$$u(1) = u.$$

Constant Temperature

Substituting for the shear in the momentum equation yields:

$$\frac{\partial}{\partial y}(\eta\frac{\partial u}{\partial y}) = \frac{\partial u}{\partial t}$$

The differential equation to solve is:

$$\frac{\partial^2 u}{\partial y^2} = \frac{1}{\eta}\frac{\partial u}{\partial t}$$

The solution of this equation will have two terms a steady state term and a transient term. The steady state solution will satisfy both boundary conditions. The transient solution must be zero at both boundaries and must decay with time.

The steady state solution solves the invariant case of the momentum equation or:

$$\frac{d^2 u}{dy^2} = 0$$

The solution of this equation is the following:

$$U_\infty = u_0\frac{y}{l}$$

For the sake of generality the transient solution should take the form:

$$U_T = \sum_{n=1}^{\infty} a_n \sin\frac{n\pi y}{l}\exp(\frac{n^2\pi^2\eta}{l^2}t)$$

where a_n is a Fourier coefficient.

At t=0 the velocity profile the velocity is zero so:

$$u = u_o \frac{y}{1} + \sum_{n=1}^{\infty} a_n \sin \frac{n \pi y}{1} = 0$$

Using the equation for sine Fourier series coefficients from Hildebrand[3]:

$$a_n = -\frac{2u_o}{1^2} \int_0^1 y \sin \frac{n \pi y}{1} dy$$

Therefore, the total solution for a constant viscosity liquid is:

$$u = u_o \frac{y}{1} + 2 u_o \sum_{n=1}^{\infty} \left[\frac{1}{n\pi} \cos n\pi - \frac{1}{1^2} \sin n\pi \right] \sin \frac{n\pi y}{1} \exp \left(-\frac{n^2 \pi^2 \eta}{1^2} t \right)$$

Variable Viscosity; Linear Temperature Gradient

The variable viscosity case is solved similar to the constant viscosity case. There are two terms in the solution, a steady state term and a transient term. The transient term for this case was not solved because of its small contribution.

The momentum equation is the same for this case as it was in the previous case:

$$\frac{\partial}{\partial y}(\tau) = \frac{\partial u}{\partial t}$$

The Newtonian shear equation is substituted into to the

momentum equation:

$$\frac{\partial}{\partial y}(\eta \frac{\partial u}{\partial y}) = \frac{\partial u}{\partial t}$$

The Absolute-Rate equation is then substituted into this equation:

$$A_1 e^{A_2/T} \frac{\partial^2 u}{\partial y^2} + A_1 A_2 \frac{1}{T^2} e^{A_2/T} \frac{\partial T}{\partial y} \frac{\partial u}{\partial y} = \frac{\partial u}{\partial t}$$

A linear expression for the temperature can be substituted into the viscosity equation.

The differential equation to solve is:

$$\frac{\partial}{\partial y}(A_1 e^{\frac{A_2}{T}} \frac{\partial u}{\partial y}) = \frac{\partial u}{\partial t}$$

The homogenous or invarient equation to solve for the steady state solution is:

$$\frac{d^2 u}{dy^2} + A_2 \frac{C_1}{(C_1 y + C_2)^2} \frac{du}{dy} = 0$$

This can be simplified by this substitution:

$$\frac{du}{dy} = z$$

it becomes:

$$\frac{dz}{dy} + \frac{A_2 C_1}{C_1^2 y^2 + 2C_1 C_2 y + C_2^2} = 0$$

The solution of which is:

$$z = \frac{A_2}{C_1 y + C_2} + C_3$$

A 4

Reversing substitution the following integral is obtained:

$$u = \int \left(\frac{A_2}{C_1 y + C_2} + C_3 \right) dy$$

The steady state solution for a linear temperature distribution is:

$$u = \frac{A_2}{C_1} \ln |(C_1 y + C_2)| + C_3 y + C_4$$

The boundary conditions:

$$u(0) = \frac{A_2}{C_1} \ln C_2 + C_4 = 0$$

$$u(l) = \frac{A_2}{C_1} \ln (C_1 l + C_2) + C_3 l + C_4 = u_\bullet$$

will be satisfied if:

$$C_3 = \frac{u_\bullet}{l} + \frac{A_2}{C_1 l} \ln(C_2) - \frac{A_2}{C_1 l} \ln(C_1 l + C_2)$$

$$C_4 = - \frac{A_2}{C_1} \ln C_2$$

Calculation of Constants For the Absolute-Rate Equation

Before these equations can be useful the two constants from the Absolute-Rate equation must be calculated. They can be taken from a graph of the ln η versus $\frac{1}{T}$. The graph should be linear satisfying the following equation:

$$\ln \eta = \ln A_1 + \frac{A_2}{T}$$

The slope of Graph 10 is 38.22 ln(Poise)·°K for the clad/rim glass and 85.66 ln(Poise)·°K for the core glass. The y-intercepts for these plots are -24.35 ln(Poise) for the clad/rim glass and -69.52 ln(Poise) for the core glass. Therefore the constants for the rim/clad glass are:

$$A_1 = e^{y-intercept} = 2.66 \cdot 10^{-11}$$
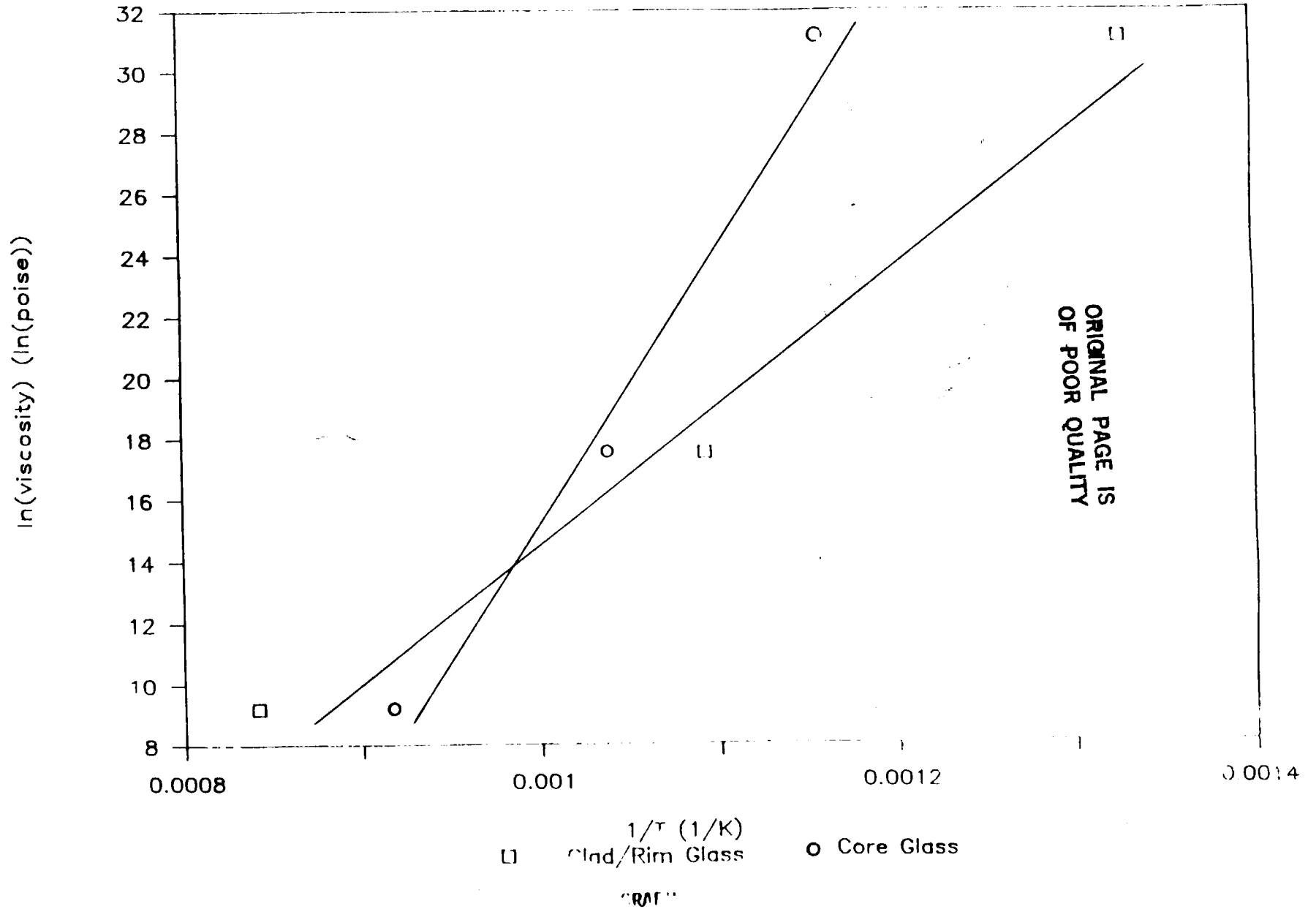$$A_2 = 38.22$$

and the constants for the core glass are:

$$A_1 = 6.42 \cdot 10^{-31}$$
$$A2 = 85.66$$

Ln(viscosity) vs. 1/T

ln(viscosity) (ln(poise)) vs. **1/T (1/K)**

□ Clad/Rim Glass	○ Core Glass

ORIGINAL PAGE IS
OF POOR QUALITY

Notation used in Equations and Derivations

u = velocity in the x direction (cm/s)

y = distance from the stationary piece of rigid glass (cm) (see figure 2)

t = time (s)

T = temperature (°K)

τ = shear stress (dynes/cm^2)

η = viscosity (g/cm·s)

l = thickness of MCP wafer (cm)

u_O = velocity of the top of the MCP (cm/s)

U_{SS} = steady state term of the velocity equation

U_T = transient term of the velocity equation

a_n = Fourier coefficient of a Fourier sine series

n = integer constant (1,2,3,...)

A_1 and A_2 = constants in the Absolute-Rate viscosity relation

C_1 and C_2 = constants in the temperature profile equation

C_3 and C_4 = integration constants

BIBLIOGRAPHY

1. Kingery, W.D., Bowen, H.K. and Uhlmann, D.R.; <u>Introduction to Ceramics</u>, John Wiley and Sons, New York, Second Edition, 1976.

2. Galileo Laboratory; Glass Optical and Physical Properties Data Sheet, June 14, 1985, Revision 4.

3. Hildebrand, F.B.; <u>Advanced Calculus for Applications</u>, Prentice Hall Inc., Englewood Cliffs, New Jersey, 1976.

4. White, Frank M.; <u>Fluid Mechanics</u>, McGraw Hill Book Company, New York, 1979.